

Quantum Metrological Power of Continuous-Variable Quantum Networks

Hyukgun Kwon,¹ Youngrong Lim,² Liang Jiang,³ Hyunseok Jeong,^{1,*} and Changhun Oh^{3,†}

¹*Department of Physics and Astronomy, Seoul National University, Seoul 08826, Republic of Korea*

²*School of Computational Sciences, Korea Institute for Advanced Study, Seoul 02455, Korea*

³*Pritzker School of Molecular Engineering, The University of Chicago, Chicago, Illinois 60637, USA*

We investigate the quantum metrological power of typical continuous-variable (CV) quantum networks. Particularly, we show that most CV quantum networks provide an entanglement between modes that enables one to achieve the Heisenberg scaling of an estimation error for distributed quantum displacement sensing, which cannot be attained using an unentangled state. In addition, we find a tolerant photon-loss rate that maintains the quantum enhancement for practical applications. Finally, we numerically demonstrate that even when CV quantum networks are composed of local beam splitters, the quantum enhancement can be attained when the depth is sufficiently large.

Quantum metrology is a study on advantages of quantum resources for parameter estimation [1–6]. In many years, nonclassical features of quantum probes have been shown to achieve a better sensitivity than any classical means. Especially in continuous-variable (CV) systems, a squeezed state, one of the most representative nonclassical states, elevates the sensitivity of optical interferometers [7, 8] including gravitational wave detectors [9–11]. In addition, enhanced phase estimation using a squeezed state has been implemented in many experiments [12–14].

More recently, besides quantum enhancement from a local system, much attention has been paid to employ a metrological advantage from entanglement between distant sites. Particularly, distributed quantum sensing has been proposed to enhance the sensitivity by exploiting quantum entanglement constituted by a quantum network for estimating a parameter in distant nodes [15–23]. For example, a single-mode squeezed vacuum state distributed by a balanced beam splitter network (BSN) was shown to enable estimating the quadrature displacement with a precision up to a Heisenberg scaling in terms of the number of modes, which cannot be achieved without entanglement [24]. Such an enhancement has also been found in distributed quantum phase sensing [19, 20, 22]. Remarkably, the enhancement from entanglement between different nodes has been experimentally demonstrated in various tasks [20, 21, 23, 25].

While particular CV quantum networks provide an enhancement for distributed sensing, it is not clear whether a general quantum network is beneficial. Since quantum entanglement between distant nodes is the key to improving the sensitivity in many cases, investigating what kinds of quantum networks are advantageous for distributed sensing is crucial for practical applications. In this paper, we show that generic CV quantum networks can be exploited to attain quantum metrological enhancement. More specifically,

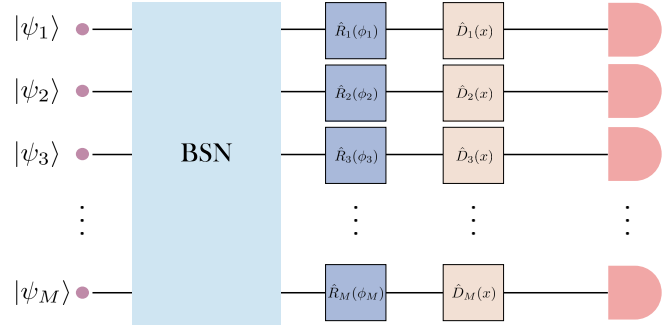


FIG. 1. Schematic of distributed quantum displacement sensing. A product state undergoes a BSN, representing a CV quantum network. We then perform local operations to prepare a probe state, which is local phase shifts $\otimes_{j=1}^M \hat{R}_j(\phi_j)$ in our scheme. A displacement parameter x of interest is then encoded onto the probe state by the displacement operator $\otimes_{j=1}^M \hat{D}_j(x)$. Finally, we measure the output state and estimate the unknown parameter using the measurement outcomes.

we prove by studying global random CV networks that most CV quantum networks except for an exponentially small fraction in the number of modes allow us to achieve the Heisenberg scaling for a distributed quantum displacement sensing scheme.

In addition, we show that local operations after an input quantum state undergoes a CV quantum network are essential for the enhancement in the sense that without them, the Heisenberg scaling cannot be attained with a high probability. We then revisit our main theorem for practical perspectives considering photon loss and find a tolerable loss amount that maintains the Heisenberg scaling. Furthermore, we numerically demonstrate that a quantum network composed of layers of local random beam splitters instead of a global random quantum network renders the Heisenberg scaling for distributed displacement sensing on average within a depth proportional to M^2 with M being the number of modes.

Distributed quantum displacement sensing.— We introduce a distributed quantum displacement sensing scheme using a CV quantum network on an M -mode

* h.jeong37@gmail.com

† changhun@uchicago.edu

CV system [24]. Our goal is to show that CV quantum networks allow a quantum enhanced estimation for such a displacement estimation task. We emphasize that our protocol can offer advantages for many quantum metrological applications [24, 26–28].

For distributed displacement sensing, we first prepare a product state and inject the state into a BSN to obtain an entangled probe. In particular, we prepare a single-mode squeezed vacuum state as an input state, squeezed along the x -axis with a mean photon number \bar{N} . The squeezed state is then injected into the first mode of the BSN to generate entanglement between M modes, with other input modes being in the vacuum. Here, a BSN is described by an $M \times M$ unitary matrix U , which transforms input annihilation operators $\{\hat{a}_i\}_{i=1}^M$ as

$$\hat{a}_i \rightarrow \hat{U}^\dagger \hat{a}_i \hat{U} = \sum_{j=1}^M U_{ij} \hat{a}_j. \quad (1)$$

After the BSN, we perform local phase shift operations, which are written as $\hat{R}(\phi) \equiv \otimes_{j=1}^M \hat{R}_j(\phi_j)$ with $\hat{R}_j(\phi_j) \equiv e^{i\phi_j \hat{a}_j^\dagger \hat{a}_j}$ being a phase shift operator on j th mode for ϕ_j . Thus, for a given BSN, a local-phase optimization can be implemented by manipulating ϕ_j 's. The entangled probe then encodes a displacement parameter x of interest. We assume that the same displacement occurs in all M modes along the same direction, the operator of which is written as $\otimes_{j=1}^M \hat{D}_j(x)$ with $\hat{D}_j(x) \equiv e^{-i\hat{p}_j x}$ being a displacement operator along x -direction. Here, we define x and p quadrature operator of j th mode as $\hat{x}_j \equiv (\hat{a}_j + \hat{a}_j^\dagger)/\sqrt{2}$, $\hat{p}_j \equiv (\hat{a}_j - \hat{a}_j^\dagger)/\sqrt{2}i$. Finally, we locally measure the output state on each site using homodyne detection and estimate the unknown parameter x using the measurement outcomes. Figure 1 illustrates our displacement distributed sensing scheme. We emphasize that in our scheme, an extra quantum network other than a BSN to generate an entangled probe is not allowed for measurement. We note that the proposed scheme is similar to the one in Ref. [24] except that we employ an arbitrary BSN instead of a balanced BSN.

Meanwhile, when we estimate a parameter θ of interest using a quantum state probe $\hat{\rho}$, the estimation error of any unbiased estimator, denoted by $\Delta^2\theta$, is bounded by the quantum Cramér-Rao lower bound as $\Delta^2\theta \geq 1/H$, where H is the quantum Fisher information (QFI) for a given system and a probe state $\hat{\rho}$ [29, 30]. Therefore, QFI quantifies the ultimate achievable estimation error using a given quantum state. Especially for a pure state probe $|\psi\rangle$ and a unitary dynamics with a Hamiltonian operator \hat{h} , the QFI can be simplified as $H = 4(\Delta^2\hat{h})_\psi \equiv 4(\langle \hat{h}^2 \rangle_\psi - \langle \hat{h} \rangle_\psi^2)$.

For distributed displacement sensing, the attainable QFI increases at most linearly in M without entanglement between modes, i.e., using a product of an identical state for M modes such as a squeezed state [24]. Remarkably, if one employs a balanced BSN to prepare an entangled state between M modes, the QFI

is shown to increase as M^2 [24], which we call the Heisenberg scaling throughout the paper. Therefore, an entanglement provides an advantage for distributed quantum displacement sensing if one prepares a suitable CV quantum network to generate entanglement. While a specific BSN is known to be beneficial for distributed quantum displacement sensing, we now show that a typical BSN enables us to achieve the Heisenberg scaling for estimating displacement.

Results.— We first derive the QFI for distributed displacement sensing for a given CV quantum network, characterized by an $M \times M$ unitary matrix U as in Eq. (1). After a BSN and phase shifters, a probe state can be written as $|\psi\rangle = \hat{R}(\phi)\hat{U}|\psi_{\text{in}}\rangle$, where $|\psi_{\text{in}}\rangle$ is a product state of a single-mode squeezed state in the first mode and $(M-1)$ vacua in the remaining modes. Since the Hamiltonian operator is $\hat{h} = \sum_{j=1}^M \hat{p}_j$, the QFI for distributed displacement estimation can be obtained as

$$H_{LO}(U) = \max_{\phi} 4(\Delta^2\hat{h})_\psi = 2M + 4 \left(\sum_{a=1}^M |U_{a1}| \right)^2 f_+(\bar{n}M), \quad (2)$$

where $\bar{n} \equiv \bar{N}/M$ is the mean photon number per mode, and we have defined $f_+(\bar{n}M) \equiv \bar{n}M + \sqrt{\bar{n}^2 M^2 + \bar{n}M}$. Here, the optimality condition of local phases for a given U is written as $e^{i\phi_a} = U_{a1}^*/|U_{a1}|$. The derivation of the QFI and the optimality condition is provided in Appendix B.

Note that since the factor $f_+(\bar{n}M)$ in Eq. (2) is order of M for fixed \bar{n} , whether the Heisenberg scaling can be achieved, i.e., $H_{LO}(U) \propto M^2$, is determined by the property of BSN U . Particularly, for a trivial BSN, namely, $U = \mathbb{1}_M$, we do not attain any entanglement from it and the QFI is linear in M . Thus, it fails to achieve the Heisenberg scaling without entanglement. On the other hand, using the Cauchy-Schwarz inequality, one may show that the QFI is maximized by a balanced BSN, i.e., $|U_{a1}| = 1/\sqrt{M}$ for all a 's, which leads to the QFI as

$$H_{\text{max}} \equiv \max_U H_{LO}(U) = 2M + 4M f_+(\bar{n}M). \quad (3)$$

Since the maximum QFI for a particular BSN achieves the Heisenberg scaling, it clearly shows the quantum enhancement from a CV quantum network and entanglement generated from it. One can also prove that H_{max} is maximal not only in our scheme but also over any quantum states with the photon-number constraint \bar{N} (See Appendix A.).

Since our goal is to show typical CV quantum networks' quantum metrological enhancement, we now compute the average QFI over random CV quantum networks using Eq. (2), i.e., random unitary matrices drawn from μ , where μ is the Haar measure on the $M \times M$ unitary matrix group, and prove the following lemma:

Lemma 1. *The average QFI over random U for distributed quantum displacement sensing using a single-*

mode squeezed state is

$$\mathbb{E}_{U \sim \mu} [H_{LO}(U)] = 2M + 4 \left[\frac{\pi}{4}(M-1) + 1 \right] f_+(\bar{n}M). \quad (4)$$

First of all, Lemma 1 shows that the average QFI over random CV quantum networks follows the Heisenberg scaling. Also, note that for a large number of modes M , the ratio of the average QFI to the maximum QFI H_{\max} approaches to $\pi/4$. Therefore, one may expect that typical CV quantum networks render a quantum metrological advantage. We prove that in fact, most of CV quantum networks offer a quantum enhancement for estimating displacement, which is presented in the following theorem:

Theorem 1. *For an M -mode CV quantum network, characterized by an $M \times M$ unitary matrix drawn from the Haar measure μ on the $M \times M$ unitary matrix group, the Heisenberg scaling of QFI can be achieved with a fraction of BSNs such that*

$$\Pr_{U \sim \mu} [H_{LO}(U) = \Theta(M^2)] \geq 1 - \exp[-\Theta(M)]. \quad (5)$$

Proof sketch. (See Appendix C for a formal proof.) From the concentration of measure inequality [31, 32], we have

$$\Pr_{U \sim \mu} \left[\left| f(U) - \mathbb{E}_{U \sim \mu} [f(U)] \right| \geq \epsilon \right] \leq 2 \exp \left(-\frac{M\epsilon^2}{4L^2} \right), \quad (6)$$

where $f : U \mapsto \mathbb{R}$ is a real function and L is its Lipschitz constant. If we let $f(U) \equiv H_{LO}(U)$ for our case, the average $H_{LO}(U)$ is given by Lemma 1. We then show that the Lipschitz constant L is upper-bounded by $8Mf_+(\bar{n}M)$. Finally, setting $\epsilon = \Theta(M^2)$ leads to Eq. (5) [33].

Since a product state renders QFI at most linear in M , Theorem 1 indicates that a typical CV quantum network with a single squeezed-vacuum state is beneficial for quantum metrology. In other words, for a randomly chosen CV quantum network except for an exponentially small fraction, the proposed distributed displacement sensing scheme achieves the Heisenberg scaling of QFI for the displacement estimation. In addition, it implies that most CV quantum networks enable one to construct an entanglement using a single-mode squeezed vacuum state because the Heisenberg scaling can only be achieved using entanglement in our scheme. Moreover, we prove that the QFIs can always be attained by performing homodyne detection along x -axis without an additional network (See Appendix E.).

While our scheme with a single-mode squeezed vacuum state in a fixed mode is sufficient for our goal, the input state can be further optimized in principle. For example, one may choose an optimal input mode for a single-mode squeezed vacuum state for a given BSN or a product of squeezed vacuum states as an input.

Furthermore, since we can achieve the Heisenberg scaling using the optimal local phase shifts ϕ^* , Theorem

1 can be interpreted from a different aspect. From the perspective of active transformation, the local phase shift for i th mode $\hat{R}_i(\phi_i^*)$ transforms the quadrature operator \hat{p}_i into $\hat{R}_i^\dagger(\phi_i^*)\hat{p}_i\hat{R}_i(\phi_i^*) = \hat{x}_i \sin \phi_i^* + \hat{p}_i \cos \phi_i^*$. Thus, if we absorb the local phase shifters into displacement operators by the above transformation, Theorem 1 implies that the QFI of a state right after a BSN mostly follows the Heisenberg scaling with respect to a parameter x generated by operators $\sum_{i=1}^M (\hat{x}_i \sin \phi_i^* + \hat{p}_i \cos \phi_i^*)$, where ϕ^* satisfies $e^{i\phi_a} = U_{a1}^*/|U_{a1}|$ for all a 's for a given BSN U . Consequently, we obtain the following corollary:

Corollary 1. *When a single-mode squeezed vacuum state undergoes a random BSN, most of the output states are beneficial for a distributed quantum displacement sensing with a specific direction of displacement.*

Thus, in general, a random BSN yields an entangled probe that has an enhancement for particular metrological tasks. Nevertheless, if we fix the direction of displacement of interest, we find that local optimization is essential for our protocol. In fact, without local operation, i.e., $\phi_a = 0$ for all a 's, we cannot attain the Heisenberg scaling even if the input state is chosen to be the optimal state that maximizes QFI for a given U . Let us denote the QFI of the optimal state as $\mathcal{H}(U)$. We can derive the following result:

Theorem 2. *Without local operation, the fraction of random BSNs that QFI attains Heisenberg scaling is almost zero even though we choose the input state as the optimal state for a given U ,*

$$\Pr_{U \sim \mu} [\mathcal{H}(U) = \Theta(M^2)] \leq \exp[-\Theta(M)], \quad (7)$$

where $\mathcal{H}(U)$ the QFI of the optimal state.

Proof sketch. First, we find the upper bound of the QFI of the optimal state for a given U when there is no local operation. We then show that the upper bound scales as M except for an exponentially small fraction of U in M , which implies that the QFI scales at most linearly in M except for an exponentially small fraction of U . The detailed proof is provided in Appendix D.

We now numerically demonstrate our results. Figure 2 exhibits QFIs averaged over 20,000 different Haar-random BSNs with a squeezed vacuum state input. As implied by Theorems 1 and 2, it clearly shows that when we optimize the local phase shifts for a given BSN, we obtain QFIs following the Heisenberg scaling as the number of modes M grows, while if we do not control the local phases, the Heisenberg scaling cannot be achieved. Here, the QFI using a single-mode squeezed state input injected into an optimal input mode without local optimization is given by (See Appendix D.)

$$H_{MO} \equiv \max_{1 \leq b \leq M} \left[2M + 4 \left| \sum_{a=1}^M U_{ab} \right|^2 f_+(\bar{n}M) \right]. \quad (8)$$

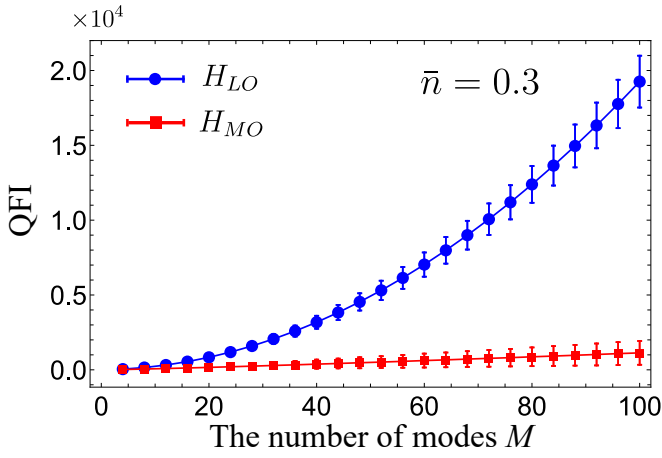


FIG. 2. QFI averaged over 20000 different Haar-random BSNs with a single-mode squeezed vacuum state input. Here, $\bar{n} = 0.3$. The blue dots represent H_{LO} , which is the QFI when we fix the input mode of a single-mode squeezed vacuum state and optimize the local phase shifts. The red dots represent the QFI when $\phi_j = 0$ for all j 's and the input mode of a single-mode squeezed vacuum state is optimized. In Appendix D, we also show that for large M limit, $H_{MO}(U)$ and $\mathcal{H}(U)$ have same behavior. The curves are guide for dots and the error bars represent three times of the standard deviation of QFIs for 20000 samples.

Although we have used a single-mode squeezed state instead of an optimal input state, the overall scaling of H_{MO} and \mathcal{H} is equal when M is large (See Appendix D). Furthermore, the standard deviation of QFIs are small for both cases, indicating that most BSNs with local-phase optimization allow the Heisenberg scaling using our scheme, while those without local-phase optimization does not.

Effect of loss.— We analyze the effect of the photon loss on the Heisenberg scaling with typical BSNs. Since photon loss is inevitable in practice, it is crucial to find a tolerable loss amount that maintains the Heisenberg scaling for applications. Photon loss can be modeled by a beam splitter with its transmittivity η . The beam splitter transforms annihilation operator as $\hat{a}_j \rightarrow \sqrt{\eta}\hat{a}_j + \sqrt{1-\eta}\hat{e}_j$, where \hat{e}_j is an annihilation operator for environment mode for all j 's [34]; thus, we assume that a photon-loss rate is constant over all modes. Since a photon-loss channel of the uniform loss rate commutes with beam splitters, our analysis includes photon loss occurring either before or after a BSN. One can easily find that in the presence of photon loss, the corresponding QFI and its expectation value over random U are degraded and that their analytical expression can be written by merely replacing $f_+(\bar{n}M)$ in Eqs. (2) and (4) by $\eta f_+(\bar{n}M)/[2(1-\eta)f_+(\bar{n}M)+1]$, which is shown in Appendix F. Using these results we can show that in the presence of loss, Theorem 1 is still valid as long as a loss rate $1-\eta$ is smaller than a threshold $\beta = \Theta(1/\bar{n}M)$ (See Appendix F.), i.e., as M increases, a loss rate has to decrease at least as $1/\bar{n}M$ to maintain the Heisenberg

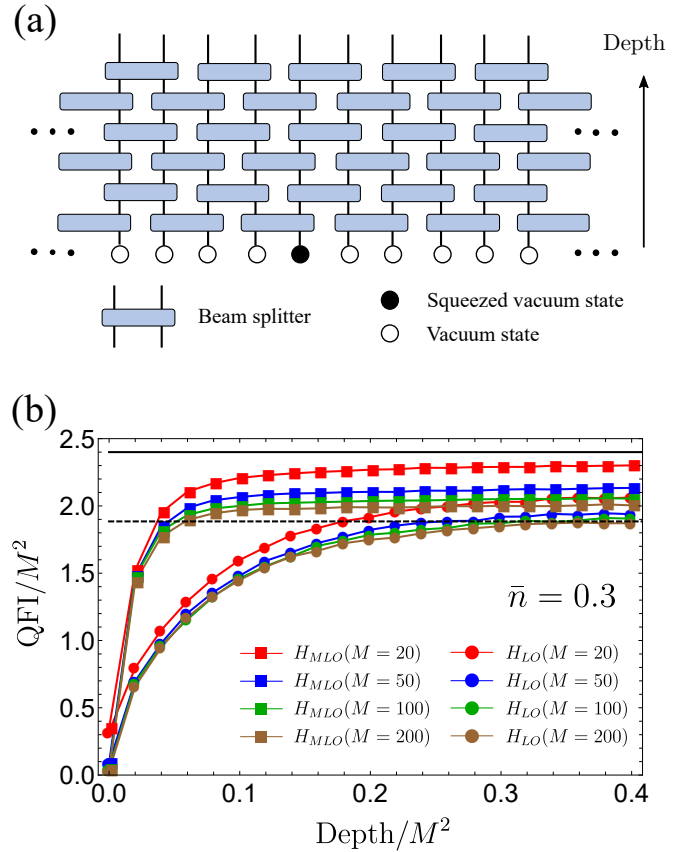


FIG. 3. (a) CV quantum network composed of local beam splitters. An input state is a single squeezed vacuum state and $(M-1)$ vacua. (b) Average QFIs over different local Haar-random beam splitters for $M = 20$ (red), 50 (blue), 100 (green), 200 (brown) with (H_{MLO}) and without (H_{LO}) optimizing the input mode of a squeezed vacuum state. The average is taken over 500, 100, 100, 50 different configurations, respectively. Here, $\bar{n} = 0.3$. Black solid line represents the asymptotic value of the maximum QFI divided by M^2 , obtained by a balanced BSN and a single squeezed vacuum state, which is equal to $8\bar{n}$. Black dashed line represents the asymptotic value of the QFI divided by M^2 , obtained by random BSN and a single squeezed vacuum state on a fixed mode, which is equal to $2\pi\bar{n}$.

scaling. We note that a CV error correction scheme for distributed quantum sensing can also be employed for practical applications [35, 36].

Local beam splitter network.— While a global random BSN is suitable to model a sufficiently complex CV network, it is also crucial to investigate how complicated the network has to be to attain a metrological enhancement from a practical perspective. To do that, we study a CV quantum network composed of a local random BSN instead of a global random BSNs[37–39], which is depicted in Fig. 3 (a). We numerically show that the Heisenberg scaling can also be achieved by using CV quantum network consisting of a local BSN. Figure 3 (b) shows the local-phase-optimized QFI with a fixed input mode and an optimized input mode for a squeezed

vacuum state. The QFI of the latter is given by (See Appendix B.)

$$H_{MLO} \equiv \max_{1 \leq b \leq M} \left[2M + 4 \left(\sum_{a=1}^M |U_{ab}| \right)^2 f_+(\bar{n}M) \right], \quad (9)$$

which is obviously equal or greater than $H_{LO}(U)$. Here, we have averaged the QFI over different quantum networks sampled from local Haar-random beam splitters. Most importantly, one can observe that the QFI divided by M^2 is almost constant for a given D/M^2 and different M 's. It implies that the Heisenberg scaling precision can be achieved on average with a depth proportional to M^2 , independent of input-mode optimization. Nevertheless, if one optimizes the input mode of a single-mode squeezed state, the Heisenberg scaling is achieved much faster than without optimization. Since they achieve the Heisenberg scaling on average, quantum networks of local beam splitters constitute sufficient entanglement on average as expected in Ref. [38]; namely, large entanglement can be obtained for a depth $D \propto M^2$.

Discussion.— We have shown that typical CV quantum networks provide a quantum enhancement for distributed quantum displacement sensing. For the purpose of our study and for simplicity, we have used a single-mode squeezed vacuum state at a fixed mode as an input to prove Theorem 1. Nevertheless, it would be a theoretically and practically interesting future work to find the optimal input state for a given BSN. Furthermore, although we have studied distributed quantum displacement sensing, it would be interesting to investigate if similar results hold for

different metrological tasks, such as multiparameter displacement estimation [21] or phase estimation [19, 20, 22].

We finally emphasize that a similar scheme has been studied in discrete-variable systems where a Haar-random quantum state has been considered for distributed sensing [31]. Interestingly, it was shown that most of random quantum states do not exhibit the Heisenberg scaling in the system although they have a large amount of entanglement. Thus, it would be an interesting future work to investigate the difference between the results in Ref. [31] and in the present work and to further demonstrate the relation between entanglement and quantum metrological advantages.

H.K. and H.J. was supported by the National Research Foundation of Korea (NRF-2019M3E4A1080074, NRF-2020R1A2C1008609, NRF-2020K2A9A1A06102946) via the Institute of Applied Physics at Seoul National University and by the Ministry of Science and ICT, Korea, under the ITRC (Information Technology Research Center) support program (IITP-2021-2020-0-01606) supervised by the IITP (Institute of Information & Communications Technology Planning & Evaluation). Y.L. acknowledges National Research Foundation of Korea a grant funded by the Ministry of Science and ICT (NRF-2020M3E4A1077861) and KIAS Individual Grant (CG073301) at Korea Institute for Advanced Study. L.J. and C.O. acknowledge support from the ARO (W911NF-18-1-0020, W911NF-18-1-0212), ARO MURI (W911NF-16-1-0349), AFOSR MURI (FA9550-19-1-0399), NSF (EFMA-1640959, OMA-1936118, EEC-1941583), NTT Research, and the Packard Foundation (2013-39273). We also acknowledge the University of Chicago's Research Computing Center for their support of this work.

Appendix A: Optimal states for distributed displacement sensing

In this Appendix, our ultimate goal is to find the optimal quantum state that maximizes the QFI for distributed displacement sensing. In our scheme, an input state is an M -mode product state whose total mean photon number is \bar{N} , which we denote as $|\psi_{\text{in}}\rangle = |\psi_1\rangle \otimes |\psi_2\rangle \otimes \cdots \otimes |\psi_M\rangle$. After the state undergoes a BSN and phase shift operation, the state becomes

$$|\psi_{\text{in}}\rangle \rightarrow |\psi\rangle = \hat{R}(\phi)\hat{U}|\psi_{\text{in}}\rangle \quad (A1)$$

where $\phi = (\phi_1, \phi_2, \dots, \phi_M)$. After these operations, displacement parameter x is encoded on the state by the displacement operator $\hat{D}(x) = \otimes_{j=1}^M e^{-i\hat{p}_j x} = e^{-i\hat{P}x}$ where $\hat{P} \equiv \hat{p}_1 + \hat{p}_2 + \cdots + \hat{p}_M$. Due to the facts that $\hat{R}(\phi)\hat{U}|\psi_{\text{in}}\rangle$ is a pure state and $\hat{D}(x)$ is an unitary operator, the QFI $H(U, \phi, |\psi\rangle)$ is 4 times of the variance of \hat{P} [40]:

$$H(U, \phi, |\psi_{\text{in}}\rangle) = 4 \left(\Delta^2 \hat{P} \right)_\psi = 4 \left(\langle \hat{P}^2 \rangle_\psi - \langle \hat{P} \rangle_\psi^2 \right). \quad (A2)$$

To find the optimal states for distributed displacement sensing, first we focus on finding the single-mode state whose variance of \hat{p} is the largest among all states having a mean photon number \bar{n} . Using the Heisenberg uncertainty relation $\Delta^2 \hat{x} \Delta^2 \hat{p} \geq 1/4$ and the mean photon number constraint $\langle \Psi | \frac{1}{2} (\hat{x}^2 + \hat{p}^2) | \Psi \rangle = \bar{n} + \frac{1}{2}$, we can derive the following inequality:

$$\langle \Psi | \hat{p}^2 | \Psi \rangle + \frac{1}{4 \langle \Psi | \hat{p}^2 | \Psi \rangle} \leq 2\bar{n} + 1. \quad (A3)$$

By simple calculation, we can get the maximum value of $\langle \psi | \hat{p}^2 | \psi \rangle$ which satisfies inequality in Eq. (A3):

$$\max_{|\Psi\rangle} \langle \Psi | \hat{p}^2 | \Psi \rangle = \frac{2\bar{n} + 1 + 2\sqrt{\bar{n}^2 + \bar{n}}}{2}. \quad (\text{A4})$$

Meanwhile, one can easily check that the variance of a rotated quadrature operator $\hat{p}' = \hat{x} \sin \theta + \hat{p} \cos \theta$ of the $|sqz(\theta, \bar{n})\rangle$ of a single-mode squeezed vacuum state, defined as $|sqz(\theta, \bar{n})\rangle = \exp\left[\frac{1}{2}r(\hat{a}^\dagger e^{-2i\theta} + \hat{a} e^{2i\theta})\right] |0\rangle$ with mean photon number is $\bar{n} = \sinh^2 r$ is written as [41]

$$\Delta^2 \hat{p}' = \langle sqz(\theta, \bar{n}) | \hat{p}'^2 | sqz(\theta, \bar{n}) \rangle = \frac{e^{2r}}{2} = \frac{2\bar{n} + 1 + 2\sqrt{\bar{n}^2 + \bar{n}}}{2}. \quad (\text{A5})$$

By using Eq. (A5), we find the optimal state. By comparing Eq. (A4) and (A5), we can ensure that a squeezed vacuum state maximizes the variance $\Delta^2 \hat{p}$.

Using the above facts, we find the state that maximizes the QFI for estimating x , or equivalently the variance of \hat{P} . Before starting our main discussion, let us show how the quadrature operators $\{\hat{x}_i\}_{i=1}^M$ and $\{\hat{p}_i\}_{i=1}^M$ transform via an M -mode BSN operator \hat{U} and a local phase shift operator $\hat{R}(\phi) = \otimes_{j=1}^M \hat{R}_j(\phi_j) = \otimes_{j=1}^M \exp(i\phi_j \hat{a}_j^\dagger \hat{a}_j)$.

Second, let us show how the quadrature operators transform via a BSN and local phase shifts. An M -mode beam splitter network operator \hat{U} transforms the operators $\{\hat{a}_i\}_{i=1}^M$, where \hat{a}_i represents annihilation operators for i th mode, as the following form:

$$\hat{a}_i \rightarrow \hat{U}^\dagger \hat{a}_i \hat{U} = \sum_{j=1}^M U_{ij} \hat{a}_j, \quad (\text{A6})$$

where U is an $M \times M$ unitary matrix. Using Eq. (A6), we can find the transformations of the quadrature operators $\hat{x}_i = (\hat{a}_i + \hat{a}_i^\dagger)/\sqrt{2}$ and $\hat{p}_i = (\hat{a}_i - \hat{a}_i^\dagger)/i\sqrt{2}$ via \hat{U} :

$$\hat{x}_i \rightarrow \hat{U}^\dagger \hat{x}_i \hat{U} = \sum_{j=1}^M \left[\left(\frac{U_{ij} + U_{ij}^*}{2} \right) \hat{x}_j - \left(\frac{U_{ij} - U_{ij}^*}{2i} \right) \hat{p}_j \right] = \sum_{j=1}^M (\hat{x}_j \text{Re } U_{ij} - \hat{p}_j \text{Im } U_{ij}), \quad (\text{A7})$$

$$\hat{p}_i \rightarrow \hat{U}^\dagger \hat{p}_i \hat{U} = \sum_{j=1}^M \left[\left(\frac{U_{ij} - U_{ij}^*}{2i} \right) \hat{x}_j + \left(\frac{U_{ij} + U_{ij}^*}{2} \right) \hat{p}_j \right] = \sum_{j=1}^M (\hat{x}_j \text{Im } U_{ij} + \hat{p}_j \text{Re } U_{ij}). \quad (\text{A8})$$

The transformations of quadrature operators via local phase shift operator are

$$\hat{x}_i \rightarrow \hat{R}^\dagger(\phi) \hat{x}_i \hat{R}(\phi) = \hat{x}_i \cos \phi_i - \hat{p}_i \sin \phi_i, \quad (\text{A9})$$

$$\hat{p}_i \rightarrow \hat{R}^\dagger(\phi) \hat{p}_i \hat{R}(\phi) = \hat{x}_i \sin \phi_i + \hat{p}_i \cos \phi_i. \quad (\text{A10})$$

Let us back to our main discussion. Noting that the mean photon number of the state is \bar{N} , we find an upper bound of the QFI as follows:

$$H(U, \phi, |\psi_{\text{in}}\rangle) = 4 \left(\Delta \hat{P} \right)^2 \leq 4 \langle \psi_{\text{in}} | \hat{U}^\dagger \hat{R}^\dagger(\phi) \hat{P}^2 \hat{R}(\phi) \hat{U} | \psi_{\text{in}} \rangle = 4 \langle \psi_{\text{in}} | \left[\sum_{a=1}^M \sum_{b=1}^M \hat{x}_b (\text{Im } e^{i\phi_a} U_{ab}) + \hat{p}_b (\text{Re } e^{i\phi_a} U_{ab}) \right]^2 | \psi_{\text{in}} \rangle \quad (\text{A11})$$

$$= 4 \sum_{b=1}^M \langle \psi_b | \left[\hat{x}_b^2 \left(\sum_{a=1}^M \text{Im } e^{i\phi_a} U_{ab} \right)^2 + \hat{p}_b^2 \left(\sum_{a=1}^M \text{Re } e^{i\phi_a} U_{ab} \right)^2 \right] | \psi_b \rangle \quad (\text{A12})$$

$$= 4 \sum_{b=1}^M R_b \langle \psi_b | \hat{x}_b^2 \sin^2 \theta_b + \hat{p}_b^2 \cos^2 \theta_b | \psi_b \rangle = 4 \sum_{b=1}^M R_b \langle \psi_b | (\hat{x}_b \sin \theta_b + \hat{p}_b \cos \theta_b)^2 | \psi_b \rangle \quad (\text{A13})$$

$$= 4 \sum_{b=1}^M R_b \langle \psi_b | \hat{p}_b'^2 | \psi_b \rangle \leq 2 \sum_{b=1}^M R_b \left(2\bar{n}_b + 1 + 2\sqrt{\bar{n}_b^2 + \bar{n}_b} \right) = 2 \sum_{b=1}^M \left| \sum_{a=1}^M e^{i\phi_a} U_{ab} \right|^2 \left(2\bar{n}_b + 1 + 2\sqrt{\bar{n}_b^2 + \bar{n}_b} \right), \quad (\text{A14})$$

where \bar{n}_b denotes the mean photon number of mode b , $R_j(\boldsymbol{\phi}) \equiv \left(\sum_{i=1}^M \text{Im} e^{i\phi_i} U_{ij}\right)^2 + \left(\sum_{i=1}^M \text{Re} e^{i\phi_i} U_{ij}\right)^2$, $\left(\sum_{i=1}^M \text{Re} e^{i\phi_i} U_{ij}\right)^2 / R_j(\boldsymbol{\phi}) \equiv \cos^2 \theta_j$ and $\left(\sum_{i=1}^M \text{Im} e^{i\phi_i} U_{ij}\right)^2 / R_j(\boldsymbol{\phi}) \equiv \sin^2 \theta_j$. To get the equalities in Eqs. (A11)-(A14), one can refer the Eqs. (A4)-(A5). If the input state $|\psi_{\text{in}}\rangle = |\psi_1\rangle \otimes |\psi_2\rangle \otimes \cdots \otimes |\psi_M\rangle$ is $|sqz(\theta_1, \bar{n}_1)\rangle \otimes |sqz(\theta_2, \bar{n}_2)\rangle \otimes \cdots \otimes |sqz(\theta_M, \bar{n}_M)\rangle$, the inequalities are saturated. From now on, we call the state that saturates the inequalities, as a proper squeezed state. Moreover, by using Eq. (A14), we can find an upper bound of the H for a given U . Particularly, once we choose an input state as a proper squeezed state, further optimization can be performed to maximize the H by adjusting local phase shifts ϕ_a 's and photon number allocation \bar{n}_b 's. Therefore, we can rewrite H as a function of U , $\boldsymbol{\phi}$ and $\bar{\mathbf{n}} = (\bar{n}_1, \dots, \bar{n}_M)$:

$$H(U, \boldsymbol{\phi}, \bar{\mathbf{n}}) = 2M + 4 \sum_{b=1}^M \left| \sum_{a=1}^M e^{i\phi_a} U_{ab} \right|^2 \left(\bar{n}_b + \sqrt{\bar{n}_b^2 + \bar{n}_b} \right) = 2M + 4M \sum_{b=1}^M p_b(\boldsymbol{\phi}) f_+(\bar{n}_b), \quad (\text{A15})$$

where $p_b(\boldsymbol{\phi}) \equiv \left| \sum_{a=1}^M e^{i\phi_a} U_{ab} \right|^2 / M$ and $f_+(x) \equiv x + \sqrt{x^2 + x}$. Note that $\sum_{b=1}^M \left| \sum_{a=1}^M e^{i\phi_a} U_{ab} \right|^2 = M$. To find an upper bound of H , we find an upper bound of $\sum_{b=1}^M p_b(\boldsymbol{\phi}) f_+(\bar{n}_b)$. Once we consider $\{p_b(\boldsymbol{\phi})\}_{b=1}^M$ as a probability distribution, (note that $0 \leq p_b \leq 1$ for all b) we can derive following inequalities :

$$\sum_{b=1}^M p_b(\boldsymbol{\phi}) f_+(\bar{n}_b) \leq f_+ \left(\sum_{b=1}^M p_b(\boldsymbol{\phi}) \bar{n}_b \right) \leq f_+ \left(\max_{b=1}^M \sum_{b=1}^M p_b(\boldsymbol{\phi}) \bar{n}_b \right). \quad (\text{A16})$$

By using the fact that $f_+(x)$ is a concave and increasing function, the first and second inequality are established. The last inequality is saturated by the following $\bar{\mathbf{n}}$. Using the photon-number constraint $\sum_{b=1}^M \bar{n}_b = \bar{N}$,

$$\sum_{b=1}^M p_b(\boldsymbol{\phi}) \bar{n}_b = p_\nu(\boldsymbol{\phi}) \left(\bar{N} - \sum_{b \neq \nu} \bar{n}_b \right) + \sum_{b \neq \nu} p_b(\boldsymbol{\phi}) \bar{n}_b = p_\nu(\boldsymbol{\phi}) \bar{N} + \sum_{b \neq \nu} p_b(\boldsymbol{\phi}) (\bar{n}_b - \bar{n}_\nu) \leq p_\nu(\boldsymbol{\phi}) \bar{N}, \quad (\text{A17})$$

where we have chosen ν to be the index that corresponds to the maximum of $\{p_b(\boldsymbol{\phi})\}_{b=1}^M$. Consequently, the ultimate upper bound of H is

$$H(U, \boldsymbol{\phi}, \bar{\mathbf{n}}) = 2M + 4 \sum_{b=1}^M \left| \sum_{a=1}^M e^{i\phi_a} U_{ab} \right|^2 f_+(\bar{n}_b) \leq 2M + 4M f_+(p_\nu(\boldsymbol{\phi}) \bar{N}) \leq 2M + 4M f_+(\bar{N}) \equiv H_{max}. \quad (\text{A18})$$

Note that all the inequalities in Eq. (A18) are saturated only when $p_\nu(\boldsymbol{\phi})$ is 1 which is the case when the BSN is balanced. A balanced BSN satisfies $e^{i\phi_a} U_{a\nu} = 1/\sqrt{M}$ for all a 's for some ν .

Appendix B: Local optimized QFI

The first step to prove Lemma 1 and Theorem 1 is to find the local-phase-optimized QFI $H_{LO}(U)$ in Eq. (2). In our scheme, we consider a single-mode squeezed vacuum state as an input state, squeezed along the x axis with mean photon number \bar{N} . More specifically, the squeezed state is injected into the first mode and other modes are in the vacuum regardless of U . (This state might not be a proper squeezed state.) The state undergoes a BSN, local phase shift operations, and displacement encoding. The corresponding QFI can be found via Eq. (A2) :

$$H(U, \boldsymbol{\phi}) = 2M + 4 \left[\left(\text{Re} \sum_{a=1}^M e^{i\phi_a} U_{a1} \right)^2 f_+(\bar{N}) + \left(\text{Im} \sum_{a=1}^M e^{i\phi_a} U_{a1} \right)^2 f_-(\bar{N}) \right] \quad (\text{B1})$$

where $f_-(x) = x - \sqrt{x^2 + x}$. We emphasize again that $H_{LO}(U)$ is the optimized QFI via local phase shift operations, i.e., $H_{LO}(U) \equiv \max_{\boldsymbol{\phi}} H(U, \boldsymbol{\phi})$. We can find an upper bound of $H(U, \boldsymbol{\phi})$ by using following inequalities :

$$H(U, \boldsymbol{\phi}) = 2M + 4 \left[\left(\text{Re} \sum_{a=1}^M e^{i\phi_a} U_{a1} \right)^2 f_+(\bar{N}) + \left(\text{Im} \sum_{a=1}^M e^{i\phi_a} U_{a1} \right)^2 f_-(\bar{N}) \right] \leq 2M + 4 \left(\text{Re} \sum_{a=1}^M e^{i\phi_a} U_{a1} \right)^2 f_+(\bar{N}) \quad (\text{B2})$$

$$\leq 2M + 4 \left| \sum_{a=1}^M e^{i\phi_a} U_{a1} \right|^2 f_+(\bar{N}) \leq 2M + 4 \left(\sum_{a=1}^M |U_{a1}| \right)^2 f_+(\bar{N}). \quad (\text{B3})$$

The first inequality holds because $f_-(N) \leq 0$ and others are straightforward to derive. Here, all of the above inequalities are saturated when all the ϕ_a 's satisfy the condition $e^{i\phi_a} = U_{a1}^*/|U_{a1}|$. Finally, we get the local optimized QFI:

$$H_{LO}(U) \equiv \max_{\phi} H(U, \phi) = 2M + 4 \left(\sum_{a=1}^M |U_{a1}| \right)^2 f_+(\bar{N}). \quad (\text{B4})$$

Note that H_{LO} is not fully optimized QFI over input states. Even if we only consider the input state as a single mode squeezed vacuum state, the QFI can be further optimized by choosing the optimal input mode depending on a given BSN instead of injecting the state into the first mode. When a squeezed vacuum state is injected into the b th mode, the corresponding QFI is given by $2M + 4 \left(\sum_{a=1}^M |U_{ab}| \right)^2 f_+(\bar{N})$. Therefore, more optimized QFI over both input mode and local phase is written as

$$H_{MLO}(U) \equiv \max_{1 \leq b \leq M} \left[2M + 4 \left(\sum_{a=1}^M |U_{ab}| \right)^2 f_+(\bar{n}M) \right], \quad (\text{B5})$$

which is always equal or greater than $H_{LO}(U)$.

Appendix C: Proof of Lemma 1 and Theorem 1

1. Proof of Lemma 1

Before presenting the proof of Lemma 1, we briefly introduce one of the methods to generate Haar-random unitary matrix. Suppose that there is a random $M \times M$ matrix Z whose components z_{ij} s are mutually independent and each of the entry follows the standard complex normal distribution $P(z_{ij})d^2z_{ij} = \frac{1}{\pi}e^{-|z_{ij}|^2}d^2z_{ij} = \frac{1}{\pi}e^{-R_{ij}^2}R_{ij}(dR_{ij})(d\theta_{ij})$ where $R = |z_{ij}|$ and θ_{ij} is argument of z_{ij} . By performing the Gram-Schmidt orthogonalization procedure as follows, one can generate $M \times M$ Haar-random unitary matrix [32].

$$U_1 = \frac{Z_1}{\|Z_1\|}, \quad U_2 = \frac{Z_2 - \langle Z_2, U_1 \rangle U_1}{\|Z_2 - \langle Z_2, U_1 \rangle U_1\|}, \quad U_3 = \frac{Z_3 - \langle Z_3, U_1 \rangle U_1 - \langle Z_3, U_2 \rangle U_2}{\|Z_3 - \langle Z_3, U_1 \rangle U_1 - \langle Z_3, U_2 \rangle U_2\|}, \quad \dots, \quad (\text{C1})$$

where U_i and Z_i are i th column vector of matrix U and Z each. Using Eq. (C1), we can express U_{a1} as $z_{a1}/\sqrt{\sum_{a=1}^M z_{a1}z_{a1}^*}$ or $R_{a1}e^{i\theta_{a1}}/\sqrt{\sum_{a=1}^M R_{a1}^2}$.

Proof of Lemma 1. Our goal is to find the expectation value of local optimized QFI, which is simplified as

$$\mathbb{E}_{U \sim \mu} [H_{LO}(U)] = \mathbb{E}_{U \sim \mu} \left[2M + 4 \left(\sum_{a=1}^M |U_{a1}| \right)^2 f_+(\bar{N}) \right] = 2M + 4f_+(\bar{N}) \sum_{a,b=1}^M \mathbb{E}_{U \sim \mu} [|U_{a1}||U_{b1}|]. \quad (\text{C2})$$

Note that the expectation value over Haar-random only cares the term $\sum_{a,b=1}^M |U_{a1}| |U_{b1}|$. Due to the procedure introduced above, we can simplify the term as

$$\sum_{a,b=1}^M \mathbb{E}_{U \sim \mu} [|U_{a1}| |U_{b1}|] = \left(\prod_{i=1}^M \int_0^\infty 2R_i dR_i e^{-R_i^2} \int_0^{2\pi} \frac{d\theta_i}{2\pi} \right) \left(\sum_{a,b=1}^M \frac{R_a R_b}{\sum_{k=1}^M R_k^2} \right) \quad (\text{C3})$$

$$= \left(\prod_{i=1}^M \int_0^\infty 2R_i dR_i e^{-R_i^2} \right) \left[\sum_{a=1}^M \left(\frac{R_a^2}{\sum_{k=1}^M R_k^2} \right) + \sum_{a \neq b}^M \left(\frac{R_a R_b}{\sum_{k=1}^M R_k^2} \right) \right] \quad (\text{C4})$$

$$= 1 + \binom{M}{2} \left(\prod_{i=1}^M \int_0^\infty 2R_i dR_i e^{-R_i^2} \right) \left(\frac{R_1 R_2}{\sum_{k=1}^M R_k^2} \right) \quad (\text{C5})$$

$$= 1 + \binom{M}{2} \left(\prod_{i=1}^{M-1} \int_0^{\frac{\pi}{2}} d\phi_i \right) (\cos \phi_1 \sin \phi_1 \cos \phi_2) \left[\prod_{k=1}^{M-1} (\sin \phi_k)^{2M-2k-1} \cos \phi_k \right] \\ \times \int_0^\infty dR 2^M (R)^{2M-1} e^{-R^2} \quad (\text{C6})$$

$$= 1 + \frac{\pi}{4} (M-1). \quad (\text{C7})$$

The equality between Eq. (C4) and (C5) holds because of the symmetry of a, b . In Eq. (C6), we adopt M -dimensional spherical coordinate [42]. We express the integral variables $\{R_a\}_{a=1}^M$ as $R_1 = (R \cos \phi_1)$, $R_2 = (R \sin \phi_1 \cos \phi_2)$, \dots , $R_{M-1} = (R \sin \phi_1 \sin \phi_2 \cdots \sin \phi_{M-2} \cos \phi_{M-1})$, $R_M = (R \sin \phi_1 \sin \phi_2 \cdots \sin \phi_{M-2} \sin \phi_{M-1})$ and corresponding Jacobian determinant is $\prod_{i=1}^M dR_i = R^{M-1} \prod_{k=1}^{M-2} (\sin \phi_k)^{M-k-1}$. Finally, the value in Eq. (C7) is deduced by the following integral table:

$$\int_0^{\frac{\pi}{2}} (\sin \phi)^{2M-2k-1} (\cos \phi) d\phi = \frac{1}{2} \left(\frac{1}{M-k} \right), \quad (\text{C8})$$

$$\int_0^{\frac{\pi}{2}} (\sin \phi)^{2M-2} (\cos \phi)^2 d\phi = \frac{\sqrt{\pi}}{4} \frac{\Gamma(\frac{2M-1}{2})}{\Gamma(M+1)}, \quad (\text{C9})$$

$$\int_0^{\frac{\pi}{2}} (\sin \phi)^{2M-5} (\cos \phi)^2 d\phi = \frac{\sqrt{\pi}}{4} \frac{\Gamma(M-2)}{\Gamma(\frac{2M-1}{2})}, \quad (\text{C10})$$

$$\int_0^\infty R^{2M-1} e^{-R^2} dR = \frac{\Gamma(M)}{2}, \quad (\text{C11})$$

where Γ is gamma function.

Hence, we complete the proof of Lemma 1 :

$$\mathbb{E}_{U \sim \mu} [H_{LO}(U)] = 2M + 4 \left[\frac{\pi}{4} (M-1) + 1 \right] f_+(\bar{N}) = 2M + 4 \left[\frac{\pi}{4} (M-1) + 1 \right] \left(\bar{n}M + \sqrt{\bar{n}^2 M^2 + \bar{n}M} \right). \quad (\text{C12})$$

2. Upper bound of Lipschitz Constant L_O of $H_{LO}(U)$

In this subsection we derive the upper bound of Lipschitz constant L_O of $H_{LO}(U)$ with the aid of a function $H_1(U)$, which we introduce below. The distance between two unitary matrices U and $U' = \exp[-iX\phi]U$ can be written as $\phi \|X\|_{HS}$ [31, 32]. Here X is an $M \times M$ Hermitian matrix and $\|X\|_{HS} \equiv \sqrt{\text{Tr}[X^\dagger X]}$. Therefore the Lipschitz constant L_f of a smooth function $f: \mathcal{U}(M) \mapsto \mathbb{R}$ is the smallest positive constant satisfying the following inequality [31, 32]:

$$\left| \frac{d}{d\phi} f(e^{-iX\phi}U) \right|_{\phi=0} \leq L_f \|X\|_{HS}. \quad (\text{C13})$$

Let us introduce a function $H_1(U) \equiv 2M + 4 \left| \sum_{a=1}^M U_{a1} \right|^2 f_+(\bar{N})$ and corresponding Lipschitz constant L_1 . Note that $H_1(U)$ is the QFI when the input state is same with $H_{LO}(U)$'s but without local operation. Exploiting Eq.

(C13), we find the upper bound of L_1 :

$$\left| \frac{d}{d\phi} H_1(e^{-iX\phi}U) \right|_{\phi=0} = 4f_+(\bar{N}) \left[\left(\sum_{a=1}^M \sum_{d=1}^M -iX_{ad}U_{d1} \right) \left(\sum_{a'=1}^M U_{a'1}^* \right) + \left(\sum_{a=1}^M \sum_{d=1}^M iX_{ad}^*U_{d1}^* \right) \left(\sum_{a'=1}^M U_{a'1} \right) \right] \quad (\text{C14})$$

$$= 8f_+(\bar{N}) \left[\sum_{d=1}^M \sum_{a=1}^M \text{Im}(Y_d U_{d1} U_{a1}^*) \right] \leq 8f_+(\bar{N}) \left(\sum_{d=1}^M |Y_d| |U_{d1}| \right) \left(\sum_{a=1}^M |U_{a1}| \right) \quad (\text{C15})$$

$$\leq 8f_+(\bar{N}) \sqrt{\sum_{d=1}^M |Y_d|^2 \sum_{d=1}^M |U_{d1}|^2} \sqrt{\sum_{a=1}^M |U_{a1}|^2 \sum_{a=1}^M 1} = 8f_+(\bar{N}) \sqrt{\sum_{d=1}^M |Y_d|^2} \sqrt{M} \leq 8f_+(\bar{N}) M \|X\|_{HS} \quad (\text{C16})$$

where $Y_d \equiv \sum_{a=1}^M X_{ad}$. The first inequality in Eq. (C16) holds from the Cauchy-Schwarz inequality. The last inequality in Eq. (C16) holds by the following fact:

$$\begin{aligned} \sqrt{\sum_{d=1}^M |Y_d|^2} &= \sqrt{\sum_{d=1}^M (X_{1d} + X_{2d} + \dots + X_{Md})(X_{1d}^* + X_{2d}^* + \dots + X_{Md}^*)} \\ &= \sqrt{M \left(\sqrt{\frac{1}{M}}, \sqrt{\frac{1}{M}}, \sqrt{\frac{1}{M}}, \dots, \sqrt{\frac{1}{M}} \right) X X^\dagger \left(\sqrt{\frac{1}{M}}, \sqrt{\frac{1}{M}}, \sqrt{\frac{1}{M}}, \dots, \sqrt{\frac{1}{M}} \right)^\top} \leq \sqrt{M} \|X\| \leq \sqrt{M} \|X\|_{HS}, \end{aligned}$$

where $\|X\| \equiv \sup_{|\psi\rangle} \frac{\|X|\psi\rangle\|}{\| |\psi\rangle \|}$. We use the fact $\|X\| \leq \|X\|_{HS}$ [31]. Finally, we can conclude that the upper bound of L_1 is $8Mf_+(\bar{N})$.

Using the upper bound of L_1 and the relation between $H_{LO}(U)$ and $H_1(U)$, we can find the upper bound of L_O . $H_{LO}(U)$ can be expressed by H_1 as $H_{LO}(U) = H_1(VU)$ where $V = \text{diag}(U_{11}^*/|U_{11}|, U_{21}^*/|U_{21}| \dots U_{M1}^*/|U_{M1}|)$ is the unitary matrix corresponding to the optimal phase shifter. Note that $H_1(U) \leq H_{LO}(U)$ for all U . Without loss of generality, assume that $H_{LO}(U') \geq H_{LO}(U)$. We then derive the following equations:

$$|H_{LO}(U') - H_{LO}(U)| = H_{LO}(U') - H_{LO}(U) = H_1(V'U') - H_1(VU) \leq H_1(V'U') - H_1(V'U). \quad (\text{C17})$$

The last inequality comes from the fact that $H_1(VU) \geq H_1(V'U)$. The above inequalities imply that the upper bound of L_O is L_1 because the distance between $V'U'$ and $V'U$ is the same as the one between U' and U . Therefore we can find that L_O is bounded as $L_O \leq 8Mf_+(\bar{N})$.

3. Proof of Theorem 1

Before proceeding the proof of Theorem 1, let us introduce concentration of measure inequality [31, 43]. For a smooth function $f: U \mapsto \mathbb{R}$ where U is drawn from a Haar measure on $M \times M$ unitary matrix group μ , the following inequalities holds [43]:

$$\Pr_{U \sim \mu} \left(\left| f(U) - \mathbb{E}_{U \sim \mu} [f(U)] \right| \geq \epsilon \right) \leq 2 \exp \left(-\frac{M\epsilon^2}{4L_f^2} \right), \quad (\text{C18})$$

where L_f is Lipschitz constant of $f(U)$.

In Theorem 1, we claim that most of the local-phase-optimized QFI attains Heisenberg scaling. We process Eq. (C18) to prove our claim:

$$\Pr_{U \sim \mu} (H_{LO}(U) \leq (2\pi\bar{n} - k)M^2) \leq \Pr_{U \sim \mu} \left(H_{LO}(U) \leq \mathbb{E}_{U \sim \mu} [f(U)] - kM^2 \right) \quad (\text{C19})$$

$$\leq 2 \exp \left(-\frac{k^2 M^5}{4L_O^2} \right) \leq 2 \exp \left(-\frac{k^2 M^3}{256f_+^2(\bar{N})} \right). \quad (\text{C20})$$

Here, we have considered $f(U)$ as $H_{LO}(U)$, used the fact that $\mathbb{E}[f(U)] \geq 2\pi\bar{n}M^2$, and set ϵ as kM^2 , where $0 < k < 2\pi\bar{n}$ is some constant. The last inequality holds because the upper bound of L_O is $8Mf_+(N)$. Adopting big Θ notation and rewrite Eq. (C20), we complete the proof of Theorem 1 :

$$\Pr_{U \sim \mu} (H_{LO} \neq \Theta(M^2)) \leq \Pr_{U \sim \mu} (H_{LO}(U) \leq (2\pi\bar{n} - k)M^2) \leq \exp(-\Theta(M)), \quad (\text{C21})$$

$$\Pr_{U \sim \mu} (H_{LO} = \Theta(M^2)) \geq 1 - \exp(-\Theta(M)). \quad (\text{C22})$$

Appendix D: Proof of Theorem 2

1. Upper bound of optimal QFI without local operation

Consider the input state that maximizes the QFI for a given U among all possible states with a mean photon number \bar{N} . Here, we consider the case when there is no local operation which means $\phi = \mathbf{0}$. We denote the corresponding QFI as $\mathcal{H}(U)$. By Eq. (A15), $\mathcal{H}(U)$ is written as

$$\mathcal{H}(U) = \max_{\bar{\mathbf{n}}} H(U, \mathbf{0}, \bar{\mathbf{n}}). \quad (\text{D1})$$

In Eq. (A18), we mentioned that the upper bound of the QFI is $2M + 4Mf_+(p_\nu\bar{N})$ where $p_\nu \equiv \max_{1 \leq i \leq M} \left| \sum_{a=1}^M U_{ai} \right|^2 / M$, which depends on U . For our proof of Theorem 2, let us define a function $\mathcal{G}_i \equiv 4M + 8\bar{N} \left| \sum_{a=1}^M U_{ai} \right|^2$. Using the above functions, the following inequalities can be derived:

$$\mathcal{H}(U) \leq 2M + 4Mf_+(p_\nu\bar{N}) = 2M + 4M \left(p_\nu\bar{N} + \sqrt{p_\nu^2\bar{N}^2 + p_\nu\bar{N}} \right) \leq 2M + 2M(4p_\nu\bar{N} + 1) = \max_i \mathcal{G}_i(U), \quad (\text{D2})$$

which are the key ingredients in the proof of Theorem 2.

We remark that in Fig. 2 of the main text we consider QFI $H_{MO}(U)$ using a squeezed vacuum state into an optimized mode without local optimization, i.e., $\phi = 0$. Using Eq. (A18), $H_{MO}(U)$ is given by

$$H_{MO}(U) \equiv \max_{1 \leq b \leq M} \left(2M + 4 \left| \sum_{a=1}^M U_{ab} \right|^2 f_+(\bar{N}) \right). \quad (\text{D3})$$

For large M limit, one can easily show that the leading orders of $H_{MO}(U)$ and $\max_i \mathcal{G}_i(U)$ are equal. Due to the sandwich theorem, one can find that in the limit of large M , $H_{MO}(U)$ and $\mathcal{H}(U)$ have the same behavior.

2. Expectation value and Lipschitz constant of $\mathcal{G}_1(U)$

In this subsection we find the expectation value of $\mathcal{G}_1(U)$ over Haar-random unitary matrix U :

$$\mathbb{E}_{U \sim \mu} [\mathcal{G}_1(U)] = 4M + 8\bar{N} \mathbb{E}_{U \sim \mu} \left[\left| \sum_{a=1}^M U_{a1} \right|^2 \right] = 4M + 8\bar{N} \mathbb{E}_{U \sim \mu} \left[\sum_{a,b=1}^M U_{a1} U_{b1}^* \right] \quad (\text{D4})$$

Note that the expectation value over Haar-random only cares the term $\sum_{a,b=1}^M U_{a1} U_{b1}^*$. As a similar procedure in Appendix C, we can find the expectation value of $\sum_{a,b=1}^M U_{a1} U_{b1}^*$ over Haar-random unitary matrix U :

$$\mathbb{E}_{U \sim \mu} \left[\sum_{a,b=1}^M U_{a1} U_{b1}^* \right] = \left(\prod_{i=1}^M \int_0^\infty 2R_i dR_i e^{-R_i^2} \int_0^{2\pi} \frac{d\theta_i}{2\pi} \right) \left(\sum_{a,b=1}^M \frac{R_a R_b e^{i\theta_a} e^{-i\theta_b}}{\sum_{k=1}^M R_k^2} \right) \quad (\text{D5})$$

$$= \left(\prod_{i=1}^M \int_0^\infty 2R_i dR_i e^{-R_i^2} \right) \left(\frac{\sum_{a=1}^M R_a^2}{\sum_{k=1}^M R_k^2} \right) = 1. \quad (\text{D6})$$

Therefore, the expectation value of $\mathcal{G}_1(U)$ over Haar-random unitary matrix U is

$$\mathbb{E}_{U \sim \mu} [\mathcal{G}_1(U)] = 4M + 8\bar{N} = (4 + 8\bar{n})M. \quad (\text{D7})$$

Additionally, following the same procedure as the one in Appendix C, one can easily find that the upper bound of Lipschitz constant L_{G_1} of function $\mathcal{G}_1(U)$ is $16\bar{n}M^2$. Note that since every entry of the Haar-random unitary matrix U has the same probability distribution [32], $\mathbb{E}_{U \sim \mu} [\mathcal{G}_1(U)] = \mathbb{E}_{U \sim \mu} [\mathcal{G}_2(U)] = \dots = \mathbb{E}_{U \sim \mu} [\mathcal{G}_M(U)]$ and $L_{G_1} = L_{G_2} = \dots = L_{G_M}$.

3. Proof of Theorem 2

In Theorem 2, we claim that if we do not apply local operations, most of the QFI cannot attain Heisenberg scaling. Therefore, we need to show that the probability that $\mathcal{H}(U)$ attains $\Theta(M^2)$ is exponentially small. Instead of directly showing that that, we take a detour. First, we use the concentration measure inequality in Eq. (C18) with respect to $\mathcal{G}_1(U)$:

$$\Pr_{U \sim \mu} (|\mathcal{G}_1(U) - (4 + 8\bar{n})M| \geq kM^{2-\delta}) \leq 2 \exp\left(-\frac{k^2 M^{5-2\delta}}{4L_{G_1}^2}\right) \leq 2 \exp\left(-\frac{k^2 M^{1-2\delta}}{1024\bar{n}^2}\right). \quad (\text{D8})$$

We set ϵ as $kM^{2-\delta}$ where k and δ are constant $k > 0$ and $0 < \delta < 1/2$. Second, using $\mathcal{H}(U) \leq \max_i \mathcal{G}_i(U)$, we set the inequalities among some probabilities. Let us denote the event $(|\mathcal{G}_i(U) - (4 + 8\bar{n})M| \geq kM^2)$ as Q_i and $(|\mathcal{G}_\nu(U) - (4 + 8\bar{n})M| \geq kM^2)$ as Q_ν . The relation between Q_ν and others is $Q_\nu \subset \bigcup_{i=1}^M Q_i$. Note that $\mathcal{G}_\nu(U)$ is one of the $\{\mathcal{G}_i(U)\}_{i=1}^M$. Therefore the following inequalities can be established:

$$\Pr_{U \sim \mu} (|\mathcal{H}(U) - (4 + 8\bar{n})M| \geq kM^{2-\delta}) \leq \Pr_{U \sim \mu} (|\mathcal{G}_\nu(U) - (4 + 8\bar{n})M| \geq kM^{2-\delta}) \leq \Pr_{U \sim \mu} \left(\bigcup_{i=1}^M Q_i \right) \quad (\text{D9})$$

$$\leq \sum_{i=1}^M \Pr_{U \sim \mu} (Q_i) = M \Pr_{U \sim \mu} (|\mathcal{G}_1(U) - (4 + 8\bar{n})M| \geq kM^2) \leq \exp\left(-\frac{k^2 M^{1-2\delta}}{1024\bar{n}^2} + \ln 2M\right). \quad (\text{D10})$$

The first inequality comes from the fact that $\mathcal{H}(U) \leq \mathcal{G}_\nu(U)$ and the equality comes from the fact that $\Pr_{U \sim \mu} (Q_i)$ is symmetric over index i . Note that the expectation values and Lipschitz constants of $\{\mathcal{G}_i(U)\}_{i=1}^M$ are all same. Finally, using the above inequalities, we complete the proof of Theorem 2:

$$\Pr_{U \sim \mu} (\mathcal{H}(U) = \Theta(M^2)) \leq \Pr_{U \sim \mu} (|\mathcal{H}(U) - (4 + 8\bar{n})M| \geq kM^{2-\delta}) \leq \exp[-\Theta(M)] \quad (\text{D11})$$

$$\Pr_{U \sim \mu} (\mathcal{H}(U) \neq \Theta(M^2)) \geq 1 - \exp[-\Theta(M)]. \quad (\text{D12})$$

Appendix E: Optimality of homodyne measurement

When estimating a single parameter θ , the error of estimation $\Delta^2\theta$ is bounded by the classical Cramér-Rao lower bound as $\Delta^2\theta \geq 1/F$, where F is the Fisher information defined as $F(\theta) = \sum_x [\partial P(x|\theta)/\partial\theta]^2 / P(x|\theta)$, where $P(x|\theta)$ is the conditional probability of obtaining an outcome x when the unknown parameter is θ [44]. When $P(\vec{x}|\theta)$ follows a multivariate normal distribution with its M -dimensional first moment vector $\vec{\mu}_{\text{cl}}$ and $M \times M$ covariance matrix Σ_{cl} , the corresponding Fisher information is written as [44, 45]

$$F = \frac{\partial \vec{\mu}_{\text{cl}}^T}{\partial\theta} \Sigma_{\text{cl}}^{-1} \frac{\partial \vec{\mu}_{\text{cl}}}{\partial\theta}, \quad (\text{E1})$$

where we have assumed that $\partial \Sigma_{\text{cl}} / \partial\theta = 0$.

Meanwhile, for an M -mode Gaussian state, characterized by its $2M$ -dimensional first moment vector $\vec{\mu}_{\text{Q}}$ and $2M \times 2M$ covariance matrix Σ_{Q} , its QFI for a parameter θ is also written as [46]

$$H = \frac{\partial \vec{\mu}_{\text{Q}}^T}{\partial\theta} \Sigma_{\text{Q}}^{-1} \frac{\partial \vec{\mu}_{\text{Q}}}{\partial\theta}, \quad (\text{E2})$$

where $\mu_i \equiv \text{Tr}[\hat{\rho}\hat{Q}_i]$ and $\Sigma_{ij} \equiv \text{Tr}[\hat{\rho}\{\hat{Q}_i - \mu_i, \hat{Q}_j - \mu_j\}]/2$ with the quadrature operator vector $\hat{Q} \equiv (\hat{x}_1, \dots, \hat{x}_M, \hat{p}_1, \dots, \hat{p}_M)$. Here, we again assumed that $\partial\Sigma_Q/\partial\theta = 0$.

When we perform homodyne detection on a Gaussian state, the output probability distribution follows a normal distribution. If we perform homodyne detection along x -axis for each mode, its output distribution follows an M -dimensional multivariate normal distribution with its first moment vector $(\mu_{\text{HD}})_i = (\mu_Q)_i$ and $(\Sigma_{\text{HD}})_{ij} = (\Sigma_Q)_{ij}$ for $1 \leq i, j \leq M$. Since the output probability distribution is a normal distribution, we can apply Eq. (E1) for our scheme. In Theorem 1, we consider a single-mode squeezed vacuum state as an input state which is squeezed along the x axis with mean photon number \bar{N} . The state is injected into the first mode and other modes are in vacuum. Here we denote the state as $|\Psi\rangle = |sqz(0, \sinh^2 r = \bar{N})\rangle \otimes |0\rangle \cdots |0\rangle$. The state undergoes beam splitter array, phase shift operation and displacement encoding in regular sequence. The state right before the measurement is $\hat{D}(x)\hat{R}(\phi)\hat{U}|\Psi\rangle$. One can easily check that when the optimal phase shifts are applied, quantum covariance matrix's $M \times M$ off-diagonal block matrix vanishes, i.e., if we write

$$\Sigma_Q = \begin{pmatrix} \Sigma_Q^{xx} & \Sigma_Q^{xp} \\ \Sigma_Q^{px} & \Sigma_Q^{pp} \end{pmatrix}, \quad (\text{E3})$$

$\Sigma_Q^{xp} = \Sigma_Q^{px} = 0$. Noting that for our case, $\partial\vec{\mu}_Q/\partial x = (1, \dots, 1, 0, \dots, 0)$, we can rewrite the QFI as

$$H = \sum_{i,j=1}^M [(\Sigma_Q^{xx})^{-1}]_{ij}. \quad (\text{E4})$$

Also, for homodyne detection, the covariance matrix becomes $\Sigma_{\text{HD}} = \Sigma_Q^{xx}$ we can find that

$$F = \sum_{i,j=1}^M [(\Sigma_Q^{xx})^{-1}]_{ij}. \quad (\text{E5})$$

Therefore, the classical Fisher information of homodyne detection is the same as the QFI, which shows that homodyne detection is optimal.

Appendix F: Effect of photon loss

Photon loss can be modeled by a beam splitter with its transmittivity η . The beam splitter transforms annihilation operator as $\hat{a}_j \rightarrow \sqrt{\eta}\hat{a}_j + \sqrt{1-\eta}\hat{e}_j$, where \hat{e}_j is an annihilation operator for environment mode for all j 's [34]. When there is photon loss, the covariance matrix of Gaussian state transforms like [47]

$$\Sigma_Q \rightarrow \eta\Sigma_Q + (1-\eta)\frac{\mathbb{1}_{2M}}{2}, \quad (\text{F1})$$

where η is normalized time. Using Eq.(E2), the QFI becomes

$$H_{LO}(U, \eta = 1) = 2M + 4 \left(\sum_{a=1}^M |U_{a1}| \right)^2 f_+(\bar{N}) \rightarrow H_{LO}(U, \eta) = 2M + 4 \left(\sum_{a=1}^M |U_{a1}| \right)^2 \left[\frac{\eta f_+(\bar{N})}{2(1-\eta)f_+(\bar{N}) + 1} \right]. \quad (\text{F2})$$

Thus, when there is photon loss, the change of QFI can be captured by

$$f_+(\bar{N}) \rightarrow \frac{\eta f_+(\bar{N})}{2(1-\eta)f_+(\bar{N}) + 1}. \quad (\text{F3})$$

Let us find the tolerable η still sustains $\mathbb{E}_{U \sim \mu} [H_{LO}(U, \eta)] = \Theta(M^2)$. We can find the bound using Taylor's theorem such that

$$\frac{\eta f_+(\bar{N})}{2(1-\eta)f_+(\bar{N}) + 1} \geq \eta f_+(\bar{N}) - 2(1-\eta)f_+(\bar{N})^2. \quad (\text{F4})$$

One can easily check that this can be larger than $\alpha f_+(\bar{N})$ with some constant $0 < \alpha < 1$ when

$$\eta \geq 1 - \frac{1 - \alpha}{1 + 2f_+(\bar{N})}. \quad (\text{F5})$$

In other words, when a loss rate $1 - \eta$ satisfies

$$1 - \eta \leq \beta, \quad \text{where} \quad \beta \equiv \frac{1 - \alpha}{1 + 2f_+(\bar{N})} = \Theta\left(\frac{1}{\bar{n}M}\right), \quad (\text{F6})$$

we have

$$\frac{\eta f_+(\bar{N})}{2(1 - \eta)f_+(\bar{N}) + 1} \geq \alpha f_+(\bar{N}), \quad (\text{F7})$$

or equivalently,

$$H_{LO}(U, \eta) = 2M + 4 \left(\sum_{a=1}^M |U_{a1}| \right)^2 \left[\frac{\eta f_+(\bar{N})}{2(1 - \eta)f_+(\bar{N}) + 1} \right] \geq 2M + 4\alpha \left(\sum_{a=1}^M |U_{a1}| \right)^2 f_+(\bar{N}). \quad (\text{F8})$$

Therefore, the Heisenberg scaling maintains when as M grows, the loss rate decreases at least as $1/\bar{n}M$.

One can also directly prove the counterpart of Theorem 1. Since the average over Haar-random matrix U and Lipschitz constant rely only on the term $|U_{a1}||U_{b1}|$, the expectation value of $H_{LO}(U, \eta)$ is

$$\mathbb{E}_{U \sim \mu} [H_{LO}(U, \eta)] = 2M + 4 \left(\frac{\pi}{4}(M - 1) + 1 \right) \frac{\eta f_+(\bar{N})}{2(1 - \eta)f_+(\bar{N}) + 1} \quad (\text{F9})$$

and the corresponding Lipschitz constant $L_O(\eta)$ is

$$L_O(\eta) = \frac{8M\eta f_+(\bar{N})}{2(1 - \eta)f_+(\bar{N}) + 1}. \quad (\text{F10})$$

Thus, the concentration measure inequality Eq. (C20) becomes

$$\Pr_{U \sim \mu} \left(\left| H_{LO}(U, \eta) - \mathbb{E}_{U \sim \mu} [H_{LO}(U, \eta)] \right| \geq kM^2 \right) \leq 2 \exp \left(-\frac{k^2 M^5}{4L_O^2(\eta)} \right), \quad (\text{F11})$$

where $k > 0$ is a constant. Note that the right-hand-side of Eq. (F11) is always exponentially small for any $0 < \eta \leq 1$. Therefore, as far as $\mathbb{E}_{U \sim \mu} [H_{LO}(U, \eta)]$ is $\Theta(M^2)$, Theorem 1 is still valid. Hence, under photon-loss satisfying the condition of Eq. (F5), the Heisenberg scaling maintains.

- | | |
|--|--|
| <p>[1] V. Giovannetti, S. Lloyd, and L. Maccone, Quantum-enhanced positioning and clock synchronization, <i>Nature</i> 412, 417 (2001).</p> <p>[2] V. Giovannetti, S. Lloyd, and L. Maccone, Quantum-enhanced measurements: beating the standard quantum limit, <i>Science</i> 306, 1330 (2004).</p> <p>[3] V. Giovannetti, S. Lloyd, and L. Maccone, Quantum metrology, <i>Phys. Rev. Lett.</i> 96, 010401 (2006).</p> <p>[4] V. Giovannetti, S. Lloyd, and L. Maccone, Advances in quantum metrology, <i>Nat. Photonics</i> 5, 222 (2011).</p> <p>[5] D. Braun, G. Adesso, F. Benatti, R. Floreanini, U. Marzolino, M. W. Mitchell, and S. Pirandola, Quantum-enhanced measurements without entanglement, <i>Rev. Mod. Phys.</i> 90, 035006 (2018).</p> | <p>[6] S. Pirandola, B. R. Bardhan, T. Gehring, C. Weedbrook, and S. Lloyd, Advances in photonic quantum sensing, <i>Nat. Photonics</i> 12, 724 (2018).</p> <p>[7] R. Demkowicz-Dobrzański, M. Jarzyna, and J. Kołodyński, Quantum limits in optical interferometry, <i>Prog. Opt.</i> 60, 345 (2015).</p> <p>[8] C. Oh, C. Lee, C. Rockstuhl, H. Jeong, J. Kim, H. Nha, and S.-Y. Lee, Optimal Gaussian measurements for phase estimation in single-mode Gaussian metrology, <i>npj Quantum Inf.</i> 5, 10 (2019).</p> <p>[9] C. M. Caves, Quantum-mechanical noise in an interferometer, <i>Phys. Rev. D</i> 23, 1693 (1981).</p> <p>[10] J. Abadie, B. P. Abbott, R. Abbott, T. D. Abbott, M. Abernathy, C. Adams, R. Adhikari, C. Affeldt,</p> |
|--|--|

- B. Allen, G. Allen, *et al.*, A gravitational wave observatory operating beyond the quantum shot-noise limit, *Nat. Phys.* **7**, 962 (2011).
- [11] J. Aasi, J. Abadie, B. Abbott, R. Abbott, T. Abbott, M. Abernathy, C. Adams, T. Adams, P. Addesso, R. Adhikari, *et al.*, Enhanced sensitivity of the ligo gravitational wave detector by using squeezed states of light, *Nat. Photonics* **7**, 613 (2013).
- [12] H. Yonezawa, D. Nakane, T. A. Wheatley, K. Iwasawa, S. Takeda, H. Arao, K. Ohki, K. Tsumura, D. W. Berry, T. C. Ralph, *et al.*, Quantum-enhanced optical-phase tracking, *Science* **337**, 1514 (2012).
- [13] A. A. Berni, T. Gehring, B. M. Nielsen, V. Händchen, M. G. Paris, and U. L. Andersen, Ab initio quantum-enhanced optical phase estimation using real-time feedback control, *Nat. Photonics* **9**, 577 (2015).
- [14] J. Yu, Y. Qin, J. Qin, H. Wang, Z. Yan, X. Jia, and K. Peng, Quantum enhanced optical phase estimation with a squeezed thermal state, *Phys. Rev. Applied* **13**, 024037 (2020).
- [15] P. Komar, E. M. Kessler, M. Bishof, L. Jiang, A. S. Sørensen, J. Ye, and M. D. Lukin, A quantum network of clocks, *Nat. Phys.* **10**, 582 (2014).
- [16] T. Baumgratz and A. Datta, Quantum enhanced estimation of a multidimensional field, *Phys. Rev. Lett.* **116**, 030801 (2016).
- [17] L. Pezzè, M. A. Ciampini, N. Spagnolo, P. C. Humphreys, A. Datta, I. A. Walmsley, M. Barbieri, F. Sciarrino, and A. Smerzi, Optimal measurements for simultaneous quantum estimation of multiple phases, *Phys. Rev. Lett.* **119**, 130504 (2017).
- [18] T. J. Proctor, P. A. Knott, and J. A. Dunningham, Multiparameter estimation in networked quantum sensors, *Phys. Rev. Lett.* **120**, 080501 (2018).
- [19] W. Ge, K. Jacobs, Z. Eldredge, A. V. Gorshkov, and M. Foss-Feig, Distributed quantum metrology with linear networks and separable inputs, *Phys. Rev. Lett.* **121**, 043604 (2018).
- [20] X. Guo, C. R. Breum, J. Borregaard, S. Izumi, M. V. Larsen, T. Gehring, M. Christandl, J. S. Neergaard-Nielsen, and U. L. Andersen, Distributed quantum sensing in a continuous-variable entangled network, *Nat. Phys.* **16**, 281 (2020).
- [21] Y. Xia, W. Li, W. Clark, D. Hart, Q. Zhuang, and Z. Zhang, Demonstration of a reconfigurable entangled radio-frequency photonic sensor network, *Phys. Rev. Lett.* **124**, 150502 (2020).
- [22] C. Oh, C. Lee, S. H. Lie, and H. Jeong, Optimal distributed quantum sensing using Gaussian states, *Phys. Rev. Research* **2**, 023030 (2020).
- [23] S.-R. Zhao, Y.-Z. Zhang, W.-Z. Liu, J.-Y. Guan, W. Zhang, C.-L. Li, B. Bai, M.-H. Li, Y. Liu, L. You, J. Zhang, J. Fan, F. Xu, Q. Zhang, and J.-W. Pan, Field demonstration of distributed quantum sensing without post-selection, *Phys. Rev. X* **11**, 031009 (2021).
- [24] Q. Zhuang, Z. Zhang, and J. H. Shapiro, Distributed quantum sensing using continuous-variable multipartite entanglement, *Phys. Rev. A* **97**, 032329 (2018).
- [25] L.-Z. Liu, Y.-Z. Zhang, Z.-D. Li, R. Zhang, X.-F. Yin, Y.-Y. Fei, L. Li, N.-L. Liu, F. Xu, Y.-A. Chen, and J.-W. Pan, Distributed quantum phase estimation with entangled photons, *Nat. Photonics* **15**, 137 (2021).
- [26] F. Grosshans and P. Grangier, Continuous variable quantum cryptography using coherent states, *Phys. Rev. Lett.* **88**, 057902 (2002).
- [27] S. Pirandola, S. Mancini, S. Lloyd, and S. L. Braunstein, Continuous-variable quantum cryptography using two-way quantum communication, *Nat. Phys.* **4**, 726 (2008).
- [28] S. Pirandola, C. Ottaviani, G. Spedalieri, C. Weedbrook, S. L. Braunstein, S. Lloyd, T. Gehring, C. S. Jacobsen, and U. L. Andersen, High-rate measurement-device-independent quantum cryptography, *Nat. Photonics* **9**, 397 (2015).
- [29] S. L. Braunstein and C. M. Caves, Statistical distance and the geometry of quantum states, *Phys. Rev. Lett.* **72**, 3439 (1994).
- [30] M. G. Paris, Quantum estimation for quantum technology, *Int. J. Quantum Inf* **7**, 125 (2009).
- [31] M. Oszmaniec, R. Augusiak, C. Gogolin, J. Kołodyński, A. Acin, and M. Lewenstein, Random bosonic states for robust quantum metrology, *Phys. Rev. X* **6**, 041044 (2016).
- [32] E. S. Meckes, *The random matrix theory of the classical compact groups*, Vol. 218 (Cambridge University Press, 2019).
- [33] We write $f(M) = \Theta(g(M))$ if $f(M)$ and $g(M)$ have the same behavior in the limit of large M .
- [34] U. Leonhardt, Quantum statistics of a lossless beam splitter: SU(2) symmetry in phase space, *Phys. Rev. A* **48**, 3265 (1993).
- [35] K. Noh, S. Girvin, and L. Jiang, Encoding an oscillator into many oscillators, *Phys. Rev. Lett.* **125**, 080503 (2020).
- [36] Q. Zhuang, J. Preskill, and L. Jiang, Distributed quantum sensing enhanced by continuous-variable error correction, *New J. Phys.* **22**, 022001 (2020).
- [37] Q. Zhuang, T. Schuster, B. Yoshida, and N. Y. Yao, Scrambling and complexity in phase space, *Phys. Rev. A* **99**, 062334 (2019).
- [38] B. Zhang and Q. Zhuang, Entanglement formation in continuous-variable random quantum networks, *npj Quantum Inf.* **7**, 33 (2021).
- [39] C. Oh, Y. Lim, B. Fefferman, and L. Jiang, Classical simulation of bosonic linear-optical random circuits beyond linear light cone, *arXiv preprint arXiv:2102.10083* (2021).
- [40] J. Liu, X.-X. Jing, and X. Wang, Quantum metrology with unitary parametrization processes, *Sci. Rep.* **5**, 8565 (2015).
- [41] G. S. Agarwal, *Quantum optics* (Cambridge University Press, 2012).
- [42] L. Blumenson, A derivation of n-dimensional spherical coordinates, *Am. Math. Mon.* **67**, 63 (1960).
- [43] G. W. Anderson, A. Guionnet, and O. Zeitouni, *An introduction to random matrices*, 118 (Cambridge university press, 2010).
- [44] S. M. Kay, *Fundamentals of statistical signal processing: estimation theory* (Prentice-Hall, Inc., 1993).
- [45] B. Porat and B. Friedlander, Computation of the exact information matrix of Gaussian time series with stationary random components, *IEEE transactions on acoustics, speech, and signal processing* **34**, 118 (1986).
- [46] C. Oh, C. Lee, L. Bianchi, S.-Y. Lee, C. Rockstuhl, and H. Jeong, Optimal measurements for quantum fidelity between Gaussian states and its relevance to quantum metrology, *Phys. Rev. A* **100**, 012323 (2019).
- [47] A. Serafini, *Quantum continuous variables: a primer of theoretical methods* (CRC press, 2017).